EFFECT OF THE HORSESHOE VORTEX SYSTEM ON THE GEOMETRY OF A DEVELOPING SCOUR HOLE AT A CYLINDER

Oscar LINK[1], Christian GOBERT[2], Michael MANHARDT[3] and Ulrich ZANKE[4]

[1] Assistant Professor, Dept. of Civil Eng., University of Concepción
(Edmundo Larenas 270, Concepción, Chile)
E-mail:olink@udec.cl
[2]Doctoral Research Fellow, Fachgebiet Hydromechanik, Technische Universität München
(Arcisstr. 21, 80333 München, Germany)
E-mail: ch.gobert@bv.tum.de, m.manhardt@bv.tum.de
[3] Professor, Fachgebiet Hydromechanik, Technische Universität München
(Arcisstr. 21, 80333 München, Germany)
E-mail: ch.gobert@bv.tum.de, m.manhart@bv.tum.de
[4] Professor, Institut für Wasserbau und Wasserwirtschaft, Darmstadt University of Technology
(Rundeturmstr. 1, 64283 Darmtadt, Germany)
E-mail: wabau@wb.tu-darmstadt.de

Experimental and numerical results on scour mechanism around a single cylindrical pier are presented and analyzed. Interaction between the horseshoe vortex and the shape of developing scour holes is explored. Therefore a clear-water scour experiment in sand with $d_{50} = 0.97$ mm was conducted. During the running experiment of 21 hours duration developing scour holes were measured by a laser distance sensor. Measurements of the sand-bed geometry on several azimuthal half-planes were conducted. On the half-planes the sand-bed showed well defined slopes distinguishing three regions with different inclinations. From these measurements, the layout of the horseshoe-vortex system can be deduced. In addition to the experiment, a Large Eddy simulation was performed in order to investigate vortex characteristics in the developing scour hole. The sand-bed geometry for the numerical model was taken from the experimental measurements. Results show that instantaneous flow fields explain the measured shape of developing scour holes, whereas the time-averaged flow field does not. The scouring mechanism in sand is discussed and compared with previous work.

Key Words : *Horseshoe vortex, Scour-hole geometry, Large Eddy simulation*

1. INTRODUCTION

An important topic in bridge hydraulics is the erosion of the bed around a bridge pier due to the flow around the pier. This leads to a scouring hole. As soon as the hole is developed, the incoming boundary layer detaches from the bed and a recirculation zone is formed in front of the pier. This leads to a very complex three dimensional flow in the scour hole. Thus, scouring mechanisms around bridge piers are hard to investigate.

One of the first experiments on detailed investigations of flow patterns in scour holes draws back to Dargahi (1987, 1990). He conducted several experiments for visualization of the vortex system around the pier using the hydrogen bubble technique. Later, Graf and Istiarto (2002) and Graf and Yulistiyanto (1998) conducted ADVP measurements of the velocity field around cylinders in plane and scoured beds. Sarker (1998) and Dey and Reikar (2007) conducted ADV measurements for the characterization of time-averaged flow fields around

a cylinder. Recently, Unger and Hager (2007) presented characteristics of the vortex in front of a half-cylinder based on PIV measurements. These works all showed that the detachment of the incoming boundary layer leads to the evolution of a complex horseshoe like vortex system around the pier.

In order to study the interaction between the vortex system and the bed geometry, Yanmaz and Köse (2007) presented surface characteristics of scouring at bridge elements. They proposed empirical relations for the estimation of the time dependent scour depth. Link (2008) conducted new detailed measurements of developing scour holes in coarse sand. Data provided in that work serves as a basis for the analysis presented in this study.

Previous works also include numerical simulations of the flow in a scour hole. For example Olsen and Kjellesvic (1998) performed a Reynolds averaged Navier-Stokes (RANS) simulation with $\kappa - \varepsilon$ model. Roulund et al. (2005) recently presented results from a RANS simulation with $\kappa - \omega$ model. In both works, the main characteristics of the horseshoe vortex measured in experiments could be reproduced by RANS. To gain a deeper insight into the dynamics of the flow, unsteady RANS and Large Eddy simulations (LES) were performed as well. Recent works include for example Ge et al. (2005) and Kirkil et al. (2008).

However, there is still a lack of understanding on the scouring mechanism since experimental and numerical evidence suggest the horseshoe vortex as the main scouring mechanism, vortices picking-up sediment particles from the scour-hole surface, while shear stresses on the scour-hole surface are in the subcritical range, i.e. entrainment of sediment should not erode the whole scoured region.

In order to provide deeper insight into the scouring mechanisms, we present and analyze in this article detailed measurements of the scour-hole topography. Furthermore, results from a Large Eddy simulation are presented. The combination of experimental and numerical data shows that coherent vortices lead to a steep bed whereas vortex shedding flattens the bed. Thus, the scouring mechanisms can only be understood if the dynamics of the vortex system are fully captured.

2. LABORATORY EXPERIMENT

2.1 Facilities and experimental conditions

Scour experiments were conducted at the Institute for Hydraulic and Water Resources Engineering of the Darmstadt University of Technology, Germany. A rectangular flume with glass side-walls, 26 m long, 2 m wide and 1 m deep was used. A 0.2 m diameter Plexiglas cylindrical pier was mounted in the middle of a working section located 16 m downstream of the flume. The employed bed material was sand with grain sizes ranging between 0.6 and 2.0 mm. 50% by mass of the sediment is finer than d50 = 0.97 mm. The natural repose angle of sediment particles ϕ is 30°.

The presented experiment was conducted over 21 hours with a section-averaged velocity um = 0.30 m/s and a flow depth of h = 0.30 m. Froude and Reynolds numbers were 0.17 and 90000, respectively. Bed shear stress was equal to 95% of the critical bed shear stress for the initiation of sediment motion at the plane sediment bed. Thus, clear water conditions were achieved.

The scour-hole radius was measured with a laser distance sensor (LDS) located inside the Plexiglas pier, with an accuracy of ±0.4 mm. The sensor was driven in the vertical direction by a step-motor with a precision of ±1/50 mm allowing the recording of vertical profiles in the scour hole. In the azimuthal half-planes, the vertical positioning system was driven by a second step-motor with an accuracy of ±1/100°, allowing the distance sensor to turn around in the scour hole, taking various vertical profiles in different azimuthal half-planes. Azimuthal half-planes were measured in 24 different directions around the pier by turning the distance sensor in steps of 15 degrees. The measured radius R_θ, vertical coordinate z_θ, and radial coordinate θ, of the sensor position were registered with a frequency of 70 Hz. Details of the experimental set-up are given in Link (2006, 2008).

2.2 Results

Figure 1 shows developing scour holes on azimuthal half-planes with θ = 0, 45, 90, 135 and 180°, after t = 1, 6, 10 and 21 hrs. The shape of the scour hole remained nearly constant during scour development. The shape consisted of three regions. Close to the cylinder, a ring shaped portion can be identified. This shape was difficult to measure with the measuring system, thus the ring shape was interpolated in Figure 1 based on our observations. Over this ring, the concave hole can be divided into a lower and an upper section, separated by a clearly distinguishable kink in the bed. Below the kink the average slope of the bed was measured to be 42°. Above the kink, the average slope is 29°.

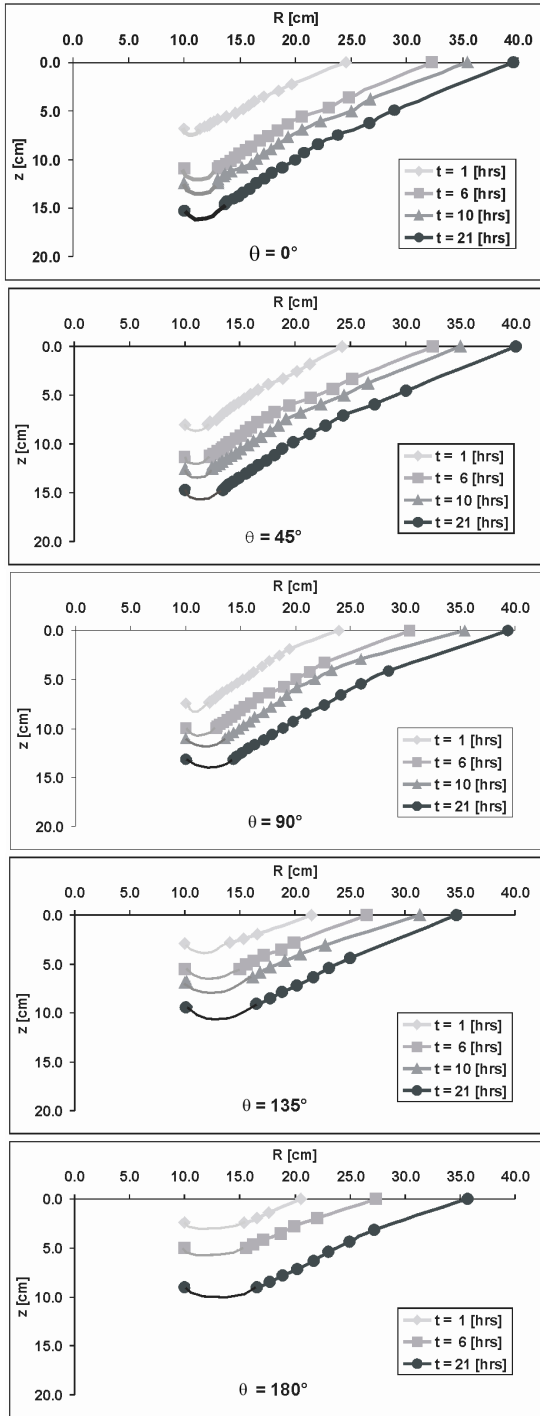The shape of the scour hole gives an idea of the flow. The different slopes suggest that the vortex

Figure 1. Developing scour holes on the azimuthal half-planes with θ = 0°, 45°, 90°, 135° and 180°. (D = 0.2 m, d50 = 0.97 mm, um = 0.3 m/s, H = 0.3 m)

system must consist of at least three vortices with different strengths, where the lower one is stronger than the upper vortex. Recirculation leads to stabilization of the bed. This could explain why the

slope of the bed can be higher than the natural repose angle. This hypothetical vortex layout is presented schematically in figure 2.
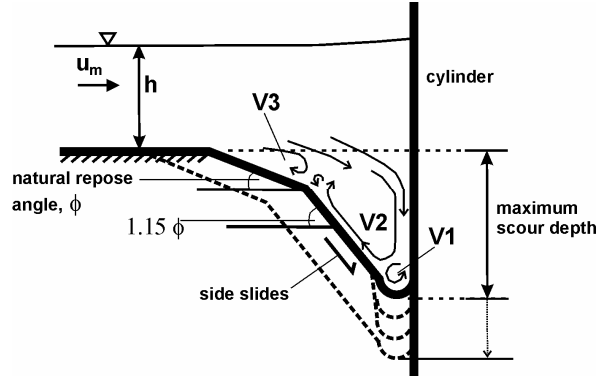

Figure 2. Suggested scouring mechanism in sand from topography measurements

3. NUMERICAL EXPERIMENT

3.1 Numerical Modelling

In order to verify the vortex system presented in figure 2 and to gain more insight into the flow field, a Large Eddy Simulation was conducted. The geometry of the developing scour hole was taken from the experimental data at t = 6 h. During the simulation the geometry was kept constant. This is justified because the time scales of the flow are very much smaller than the time span within which a significant change in the bathymetry can be observed.

The computational domain measures 5 m x 2 m x 0.3 m in streamwise, spanwise and vertical direction, respectively. The bridge pier was placed 2 m downstream from the inlet.

In spanwise direction periodic boundary conditions were implemented. On the water surface a free slip condition was imposed. Inflow conditions were taken from a periodic open channel flow of 3 m length at identical Reynolds number. At the outlet, a Dirichlet boundary condition for the pressure and von Neumann boundary conditions for the velocity components were imposed.

The flow was computed by solving the incompressible Navier-Stokes equations on a staggered grid with a second order finite volume method. For advancement in time, a third order Runge-Kutta scheme was used. For obtaining a divergence free field, the Poisson equation for the pressure was solved using the iterative solver presented by Stone (1968). These standard methods are discussed for example in Ferziger and Peric

(1996).

As LES-model, the dynamic Lagrangian Smagorinsky model proposed by Meneveau et al. (1996) was chosen. Outside the scour hole, the wall model proposed by Werner and Wengle (1991) was used. The scour hole and the bridge pier were discretized using a conservative version of the immersed boundary method described by Peller et al. (2006). Further details of the numerical method can be found in Manhart (2004).

The grid is Cartesian and equidistant in the scour hole. Here, the dimensions of the cells are 5 mm x 5 mm x 1 mm in streamwise, spanwise and vertical direction respectively. Above the scour hole, the grid was coarsened in vertical direction such that the topmost cell is 4 mm high. Based on the friction velocity at the inlet, the cell height varies between 15 wall units at the scour hole and 52 wall units at the flow surface. Towards the inlet and outlet, the grid was coarsened in streamwise direction. The length of the cells in streamwise direction at the inlet is 26 mm, at the outlet it is 55 mm. Altogether the grid consists of 21 Mio. cells. Figure 3 shows the discretisation of the computational domain.
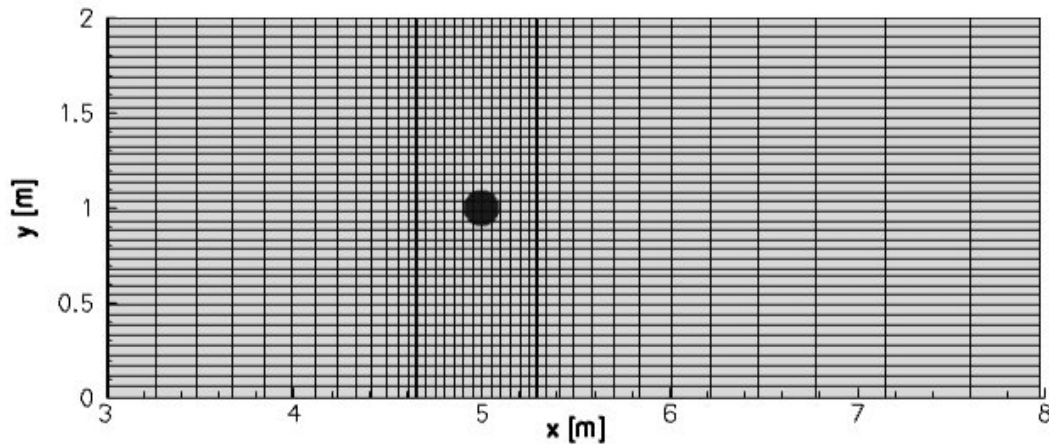

Figure 3. Computational grid (only every 10th grid point is shown)

3.2 Results

In figure 4 streamlines and pressure distribution from instantaneous fields at $\theta = 0$ are shown. In these fields, 3 to 4 vortices can be identified. The two vortices close to the pier are called herein V1 and V2 (cf. figure 4).

From animations we found that the most stable vortex is V2. This vortex is trapped in the scour hole and can be observed at almost every instant.

The small vortex V1 very close to the pier is much less stable than V2. The vortices were also analyzed with respect to the Q criterion presented by Hunt et al. (1988). This analysis showed that the rotation rate in relation to the strain rate is much higher in V2 than in V1.

V1 and V2 are counterrotating. V2 rotates such that the flow near the bed points upstream whereas the flow near the bed below V1 points downstream. This explains the shape of the bed in these sections: At V2, the inclination of the bed is higher than the repose angle because V2 transports sediment upstream whereas at V1 the bed is flat because V1 transports downstream.

Upstream of V2, more vortices can be identified. These vortices behave in an irregular way. From animations it is observed that they are formed at the detachment point of the incoming boundary layer. At this point, irregular vortex shedding can be observed. The vortices formed here are convected downstream and either interact with V2 or dissipate before they reach V2. Again, the bathymetry can be explained from these observations: The vortices which are created upstream of V2 are weaker and not as stable as V2. Thus, they can not support the sediment as strongly as V2 does and therefore the inclination of the bed upstream of V2 is smaller than the inclination at V2.

Figure 5 shows the time averaged flow field. Here, two vortices can be distinguished. These can be identified with V2 and V3 from the schematic layout in figure 1. V1 can not be observed in the time averaged flow field. From the previous analysis of the instantaneous fields it can be concluded that V3 is not a stable vortex. One might even conclude that V3 is only an artifact of averaging because the instantaneous fields showed that in this region frequent vortex shedding and detachment takes place, a process that is hidden by time averaging.
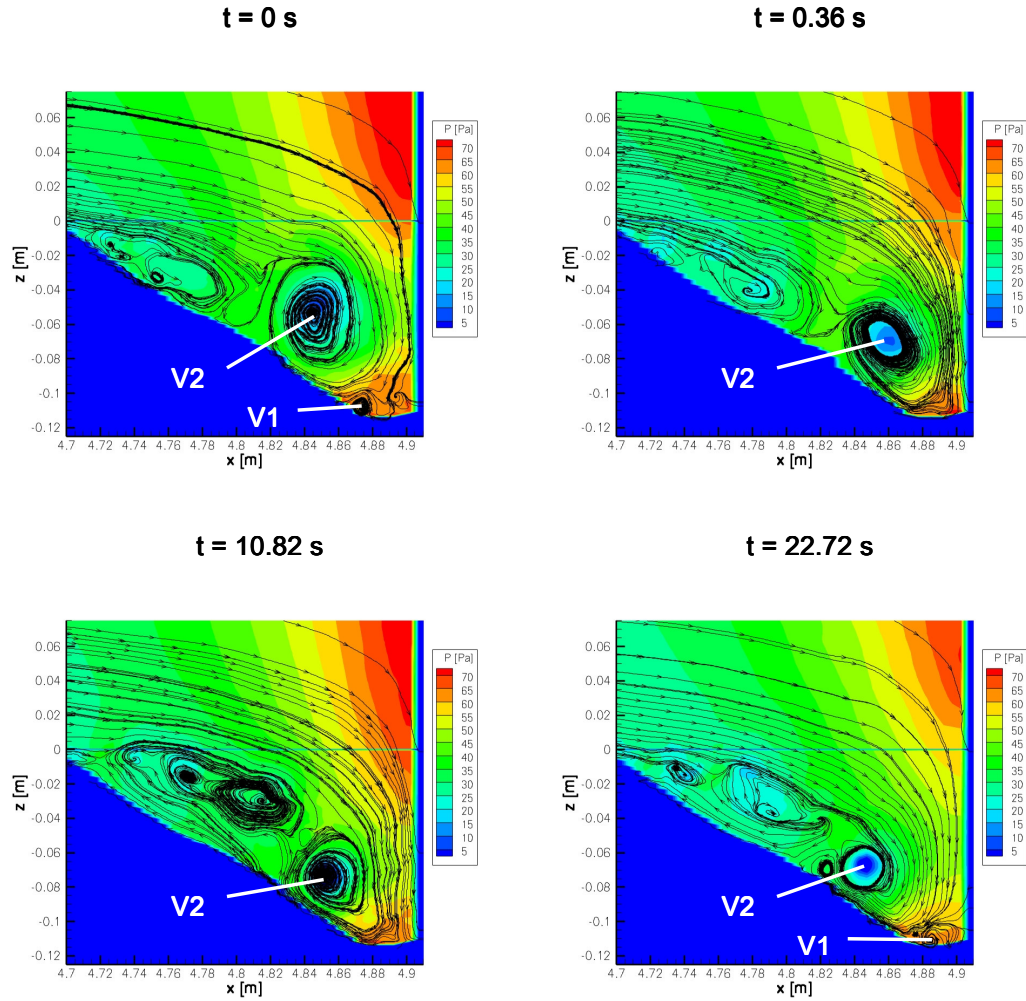
165

t = 0 s

t = 0.36 s

t = 10.82 s

t = 22.72 s

Figure 4. Streamlines and pressure (instantaneous fields) at θ = 0° and t = 0, 0.36, 10.82, and 22.72 s
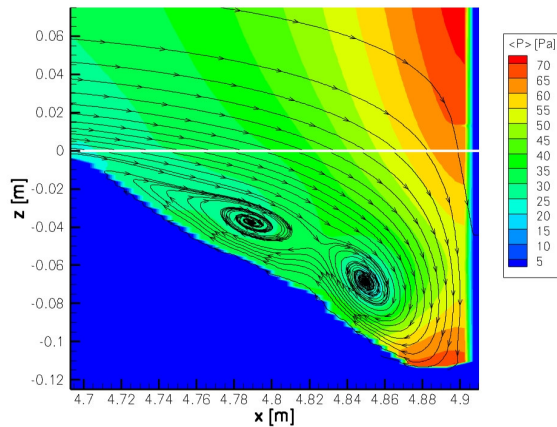
Figure 5. Streamlines and pressure (time averaged fields) at $\theta = 0°$

4. DISCUSSION

The results presented here were compared with results presented in other works on this topic. Recently, Kirkil et al. (2008) conducted a LES of a similar configuration. It is very interesting to compare their results to the results presented above because in both works laboratory experiments and Large Eddy simulations were performed. Thus, the following discussion will focus on the comparison with their work.

Kirkil et al. (2008) investigated the scouring process at a much lower Reynolds number and with different sediment. In their case, the Reynolds number based on bulk velocity and flow depth was Re=18000 (here: Re=90000), the Reynolds number based on cylinder diameter and bulk velocity was Recyl=16200 (here: Recyl=60000). Their sediment was sand with a mean diameter of 0.68 mm. Due to the difference in Reynolds number and different sediment, it is not surprising that their findings vary in some points from ours.

Furthermore, Kirkil et al. (2008) investigated the flow in the scour hole at equilibrium conditions, i.e. the bathymetry does not evolve in the experiment whereas in the present work, the geometry did not reach equilibrium conditions yet.

Kirkil et al. (2008) found two stable vortices. One can be identified with V2. The fact that in the present work no second stable vortex was observed might be due to the higher Reynolds number since

vortex shedding is more frequent at the higher Reynolds number. Thus, one might speculate that the kink in the bed might also be an effect of the Reynolds number.

The differences mentioned above can also be observed in the mean flow. Kirkil et al. (2008) found four vortices in the averaged field. The two largest vortices can be identified with the two vortices from figure 5. However, in the work of Kirkil et al., V3 is located much closer to the detachment point of the incoming boundary layer than in figure 5. This might be a result of the vortex shedding at the detachment point. In consistency with the different flow fields, Kirkil et al. (2008) also found a different bathymetry. They could not observe a change in inclination from the upper part of the scour hole to the lower part.

Vortex shedding cannot be observed from averaged fields. This shows again that it is hard to explain the bathymetry from averaged fields alone. Furthermore the averaged fields would not explain why close to the pier the surface is almost flat because in figure 5 the small vortex V1 is not observable. As discussed above, the instantaneous fields provide a possible explanation.

5. CONCLUSION

An experimental and numerical investigation of the effect of the horseshoe vortex system on the geometry of a developing scour hole at a cylinder has been presented.

Interaction between the horseshoe vortex and the shape of developing scour holes was explored through a clear-water scour experiment where topography measurements of scour holes were conducted using a laser distance sensor. From the measurements the layout of the so called horseshoe-vortex system can be deduced.

Vortex characteristics in the developing scour hole have been investigated by Large Eddy simulation. It was possible to explain the shape of the scour hole measured in the experiment from the instantaneous flow fields computed in numerical simulation.

Previous results were compared with those obtained in the present study. Results provide evidence that the dynamics of the vortex system determine the shape of the scour hole and vice versa. Therefore we propose to analyze the flow field in the scour hole further by experimental measurement of the flow and highly resolved numerical simulation.

REFERENCES

1) Dargahi, B.: Flow field and local scouring around a cylinder. Bulletin Nr. TRITA-VBI-137. The Royal Institute of Technology. Stockholm, Sweden, pp. 230, 1987.

2) Dargahi, B.: Controlling mechanism of local scouring. Journal of Hydraulic Engineering. Vol. 116. Nr. 10. pp: 1197-1214, 1990.

3) Dey, S. and Raikar, R.: Characteristics of Horseshoe Vortex in Developing Scour-holes at Piers. J. of Hydraulic Engineering, 133(4): 399-413, 2007.

4) Ferziger, J.H. and Peric, M.: Computational Methods for Fluid Dynamics. Springer: Berlin, 1996.

5) Ge, L., Lee, S., Sotiropoulos, F. and Sturm, T.: 3D unsteady RANS modeling of complex hydraulic engineering flows. I: Numerical model. J. Hydraul. Eng., 131(9): 800-808, 2005

6) Graf, W. and Istiarto, I. : Flow pattern in a scour hole around a cylinder. Journal of Hydraulic Research. Vol. 40. Nr. 1. Seiten: 13-20, 2002.

7) Graf, W. y Yulistiyanto, B.: Experiments on flow around a cylinder; the velocity and vorticity field. Journal of Hydraulic Research. Vol. 36. Nr. 4. pp: 637-653, 1998.

8) Hunt, J. C. R., Wray, A. A. and Moin, P.: Eddies, stream, and convergence zones in turbulent flows. Center for Turbulence Research Rep. CTR-S88, 1988

9) Kirkil, G., Constantinescu, S. and Ettema, R.: Coherent Structures in the Flow Field around a Circular Cylinder with Scour Hole. J. of Hydraulic Engineering, 134(5), pp: 572-587, 2008.

10) Link, O.: An investigation on scouring around a single cylindrical pier in sand. (in german). Mitteilungen des Institutes für Wasserbau und Wasserwirtschaft der Technischen Universität Darmstadt, Heft 136, pp:117, 2006.

11) Link, O.: Medición del desarrollo espacio-temporal de la socavación local alrededor de un cilindro hincado en un lecho de arena gruesa. Revista Ingeniería Hidráulica en México, Vol. XXIII, Nr. 2, 2008.

12) Manhart, M.: A zonal grid algorithm for DNS of turbulent boundary layers. Computers and Fluids, 33(3):435-461, 2004.

13) Meneveau, C., Lund, T. S. and Cabot, W. H.: A Lagrangian dynamic subgrid-scale model of turbulence. J. Fluid Mech., 319, pp: 353-385, 1996.

14) Olsen, N. and Kjellesvic, H.:Three-dimensional numerical flow modeling for estimation of maximum local scour depth. J. of Hydraulic Research, 36(4): 579-590, 1998.

15) Peller, N., le Duc, A., Tremblay, F. and Manhart, M.: High-order stable interpolations for immersed boundary methods. Int. J. Numer. Meth. Fluids, 52: 1175-1193, 2006.

16) Roulund, A., Sumer, M., Fredsøe, J. and Michelsen, J.: Numerical and experimental investigation of flow and scour around a circular pile. J. Fluid Mech., 534: 351-401, 2005.

17) Sarker, A.: Flow measurement around scoured bridge piers using Acoustic-Doppler Velocimeter (ADV). Flow Measurement and Instrumentation. Elsevier. Nr. 9: 217-227, 1999.

18) Stone, H. L.: Iterative Solution of Implicit Approximations of Multidimensional Partial Differential Equations. SIAM Journal on Numerical Analysis, 5(3): 530-558, 1968.

19) Unger, J. y Hager, W.: Down-flow and horseshoe vortex characteristics of sediment embedded bridge piers. Experiments in Fluids. Vol. 42. pp: 1-19, 2007.

20) Werner, H. and Wengle, H.: Large-eddy simulation of turbulent flow over and around a cube in a plate channel. In: 8th Symposium on Turbulent Shear Flows. pp. 155–168, 1991

21) Yanmaz, M. and Köse Ö.: Surface Characteristics of Scouring at Bridge Elements". Turkish J. Eng. Env. Sci, Vol. 31, pp. 127-134, 2007.